

## Sub-cycle electron control in the photoionization of xenon using a few-cycle laser pulse in the mid-infrared

**B Bergues**<sup>1,3</sup>, **S Zherebtsov**<sup>1</sup>, **Y Deng**<sup>1</sup>, **X Gu**<sup>1</sup>, **I Znakovskaya**<sup>1</sup>,  
**R Kienberger**<sup>1</sup>, **F Krausz**<sup>1,2</sup>, **G Marcus**<sup>1</sup> and **M F Kling**<sup>1,3</sup>

<sup>1</sup> Max-Planck-Institut für Quantenoptik, Hans-Kopfermann-St. 1,  
D-85748 Garching, Germany

<sup>2</sup> Fakultät für Physik, Ludwig-Maximilians-Universität München,  
Am Coulombwall 1, D-85748 Garching, Germany

E-mail: [boris.bergues@mpq.mpg.de](mailto:boris.bergues@mpq.mpg.de) and [matthias.kling@mpq.mpg.de](mailto:matthias.kling@mpq.mpg.de)

*New Journal of Physics* **13** (2011) 063010 (7pp)

Received 6 December 2010

Published 8 June 2011

Online at <http://www.njp.org/>

doi:10.1088/1367-2630/13/6/063010

**Abstract.** Using few-cycle laser pulses generated by optical parametric chirped pulse amplification, sub-cycle light-wave control of electrons was achieved at a carrier wavelength of 2.1  $\mu\text{m}$ . We demonstrate the sub-cycle light-wave control in the case of strong field ionization of xenon atoms. Angle-resolved spectra of electrons emitted in the photoionization process were recorded as a function of the carrier-envelope phase (CEP) using an electron imaging technique. We observed a clear CEP-dependent asymmetry in the electron momentum distribution.

In the last decade, the development of laser sources generating intense, near single-cycle infrared (IR) light pulses opened up a new horizon for time-resolved studies of the ultrafast processes that take place on attosecond ( $1 \text{ as} = 10^{-18} \text{ s}$ ) time scales, i.e. the time scales of electronic motion in atoms and molecules [1, 2]. Insights into the electron dynamics taking place in atoms exposed to such a strong laser pulse have come from the classical three-step model [3], in which first an electron is tunnel-ionized from the atom near the maximum electric field with zero momentum. Depending on the exact phase of the laser field at the moment of ionization, the electron may be driven back and may re-collide with its parent ion with a kinetic energy  $E_k$  that can reach up to  $3.17 U_p$ , where  $U_p \propto I\lambda^2$  is the cycle-averaged quiver energy of a free electron in the laser field,  $I$  the peak intensity of the laser field and  $\lambda$  the carrier wavelength. The interaction

<sup>3</sup> Authors to whom any correspondence should be addressed.

of the re-colliding electron with the parent ion can be divided into different processes: one possible process is elastic scattering of the electron with its parent ion, which gives rise to a typical electron spectrum known as the high-order above-threshold ionization spectrum [4]. Another possible process is inelastic electron scattering via the excitation or ionization of the parent ion [3]. Finally, the electron can also recombine with its parent ion while emitting the excess energy in the form of a photon having an energy  $E_{\text{ph}} = I_p + E_k$ , where  $I_p$  is the ionization potential of the atom. This process gives rise to the generation of attosecond extreme ultraviolet (XUV) bursts [5, 6].

Each of these interaction pathways allows for fascinating applications. Elastic electron scattering, for instance, can be used for time-resolved electron diffraction on molecules with Ångström spatial resolution [7] and potentially attosecond time resolution. Another application is the time-resolved study of relaxation processes initiated either with an attosecond XUV pulse [8] or via inelastic electron scattering [9]. In order to achieve electron energies high enough to excite/ionize atoms/molecules, or even make inner-shell excitation possible, high electron energies are required. Because of target depletion beyond the saturation intensity, the maximum electron energy achievable at a carrier wavelength of 800 nm, at which near single-cycle pulses are becoming routinely available [10], is limited. One way to increase  $U_p$  without entering the saturation regime is by increasing the carrier wavelength.

To control the timing of the electron–core interaction, it is essential, for few-cycle pulses, to control not only the pulse duration but also the carrier-envelope phase (CEP), defined as the phase between the maximum of the pulse envelope and the maximum of the electric field. If not stabilized, the CEP is changing from pulse to pulse and the electric field is not well defined. Nowadays, the most common way to stabilize the CEP is achieved by actively managing the dispersion inside the laser oscillator with feedback loops [11–14]. Such a stabilization approach, however, introduces instabilities into the operation of the oscillator, thus making long CEP-dependent measurements (i.e. of a few hours) difficult.

In this paper, we report on a proof of principle experiment in which the CEP dependence of the strong-field photoionization of xenon is studied at a wavelength of 2.1  $\mu\text{m}$  using an electron imaging technique [15]. According to the classical model [3], the final momentum of an electron emitted in the photoionization process is determined by the phase of the electric field at the time of ionization. For few-cycle pulses, ionization preferentially takes place within a short time window around the strongest peaks of the electric field. Controlling the CEP allows us to control the position of the maximum of the electric field with respect to the pulse envelope with sub-femtosecond precision, and in turn the final momentum of the emitted electrons.

Details of the laser source used in the present experiment can be found elsewhere [16]. Briefly, our home-built few-cycle IR light source is based on three optical parametric chirped pulse amplification (OPCPA) stages pumped by an optically synchronized 50 ps, 11 mJ Nd : YLF laser. The IR seed for the OPCPA is generated by difference frequency (DF) mixing of the ‘blue’ and the ‘red’ spectral components from a spectrally broadened Ti : sapphire laser pulse to an output spectrum centered around 2.1  $\mu\text{m}$ . This frequency mixing involves mixing the  $n$ th and the  $m$ th components in the red and blue wings of the wide-band frequency comb, respectively. The difference comb frequency can be written as  $f_{m-n} = f_m - f_n = (mf_r + f_{\text{CEP}}) - (nf_r + f_{\text{CEP}}) = (m - n)f_r$  (see figure 1). From this equation we can see that the carrier-offset frequency is canceled; thus, the CEP of the resulting DF signal is passively stabilized without the need for an active feedback loop [17]. Here we show that such a stabilization scheme significantly simplifies CEP-dependent measurements, allowing for longer measurements. The generated

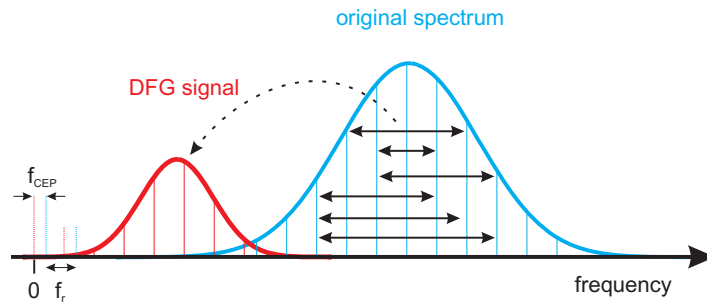


**Figure 1.** The principle of passive CEP stabilization. The carrier-offset frequency  $f_{\text{CEP}}$  cancels out in the difference frequency generation (DFG), resulting in a stable CEP.

seed is then stretched with a pair of gratings and an acousto-optic dispersive filter (Dazzler) to  $\sim 50$  ps. The  $\sim 50$  ps,  $740 \mu\text{J}$  output of the OPCPA system can be compressed to 20 fs (FWHM) ( $\sim$ two to three cycles) by letting the pulses propagate through a 10 cm-long silicon rod. After compression we obtain linearly polarized few-cycle laser pulses with an energy of  $\sim 350 \mu\text{J}$  and a repetition rate of 1 kHz. To vary the CEP, we inserted a pair of fused silica wedges into the beam path. As the laser pulse propagates through the material, the velocity difference between the carrier wave (traveling with the phase velocity) and the pulse envelope (traveling with the group velocity) induces a shift of the CE phase, which is proportional to the glass thickness. Note that  $x$  is varied only by tens of micrometers such that the induced group delay dispersion is small and does not affect the pulse duration. The pulses are sent through an adjustable iris to vary the intensity and are focused to a spot size of  $\sim 100 \mu\text{m}$  in the center of a velocity map imaging (VMI) spectrometer with an  $f = 30$  cm  $\text{CaF}_2$  lens.

The focal size was estimated using Gaussian beam propagation on the ground of the known aperture diameter and the  $M^2$  parameter of the laser beam that was determined separately by a knife-edge scan. The temporal pulse profile was characterized using a home-built third-order frequency-resolved optical gating (FROG) device [16]. The third-harmonic signal is generated on an air– $\text{CaF}_2$  interface, which possesses a large bandwidth sufficient to support the full spectrum of the amplified IR signal. A home-written FROG retrieval code is used to retrieve the pulse intensity and phase. The retrieved phase is fed back to the Dazzler to further correct for all residual dispersion. We estimate that for the present experiment the intensity in the focus was of the order of  $1 \times 10^{13} \text{ W cm}^{-2}$ .

A detailed description of the VMI used in this experiment can be found in [18]. The operating mode of the apparatus is summarized here in figure 2. Xenon gas is fed into the experimental chamber via an effusive gas jet entering the spectrometer at the tip of a shaped repeller electrode and crossing the laser beam at right angles. Electrons emitted in the interaction volume are accelerated by the electron optics towards a position-sensitive detector consisting of a pair of multi-channel plates and a phosphor screen. An electron arriving at the detector gives rise to a light flash on the phosphor screen at the impact position. A 12-bit CCD camera is used to integrate the detector signal over many laser shots. The raw image measured with the spectrometer is the orthogonal projection of the momentum distribution of the electron along the spectrometer axis.

The polarization of the laser field (the  $y$ -axis) was chosen parallel to the detector plane, such that the symmetry axis of the momentum distribution is perpendicular to the projection

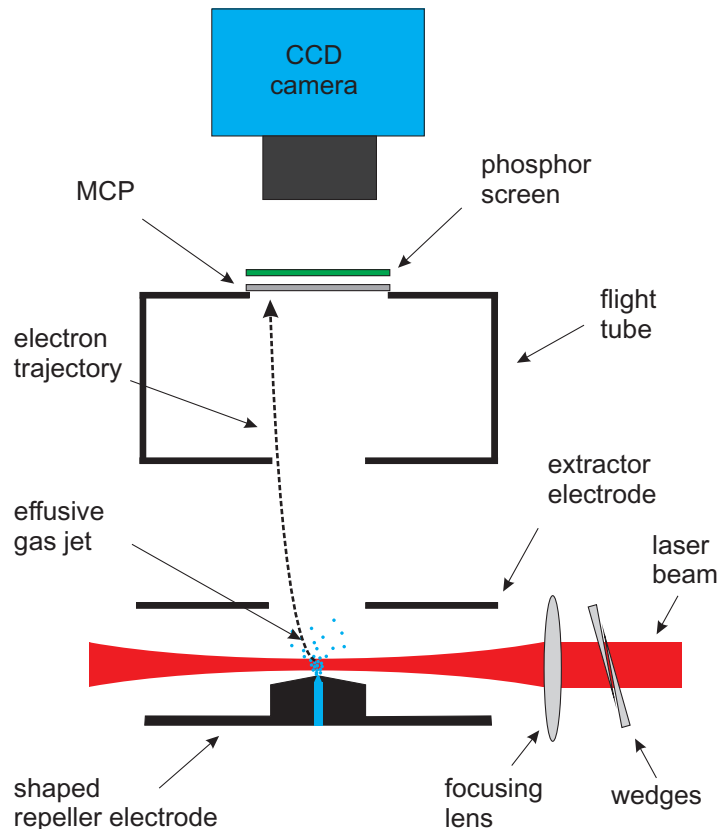


**Figure 2.** Schematic view of the experimental setup.

direction. Using the rotational symmetry of the momentum distribution about the  $y$ -axis, the full three-dimensional (3D) momentum distribution is recovered by inverse Abel transformation of the raw data using the ‘onion-peeling’ algorithm [19].

In order to investigate the effect of CEP on the ionization dynamics, we recorded a sequence of photoionization spectra of xenon for different CEPs covering a range of  $6\pi$ . For each spectrum the CEP was incremented by  $0.2\pi$  via a pair of wedges. In figure 3, we show the photoionization spectrum obtained after processing the raw data and averaging over the CEP. Here,  $p_{\parallel}$  and  $p_{\perp}$  represent the momentum components parallel to and perpendicular to the laser polarization, respectively. The spectrum exhibits features similar to those reported for strong field ionization with a few-cycle pulse at a carrier wavelength of 760 nm [20]. The electrons are emitted preferentially along the polarization direction where the spectrum extends up to a momentum of 1 a.u. The high-energy part of the spectrum beyond 0.8 a.u. consists of a characteristic hump, which is well known from the strong field ionization spectra of xenon recorded at other wavelengths, and which arises from the laser-driven elastic re-scattering of electrons from their parent ions [20].

In order to quantify the influence of the CEP on the spectra, we use the asymmetry parameter

$$A(|p_{\parallel}|, \phi_{\text{CEP}}) = \frac{N(|p_{\parallel}|, \phi_{\text{CEP}}) - N(-|p_{\parallel}|, \phi_{\text{CEP}})}{N(|p_{\parallel}|, \phi_{\text{CEP}}) + N(-|p_{\parallel}|, \phi_{\text{CEP}})},$$

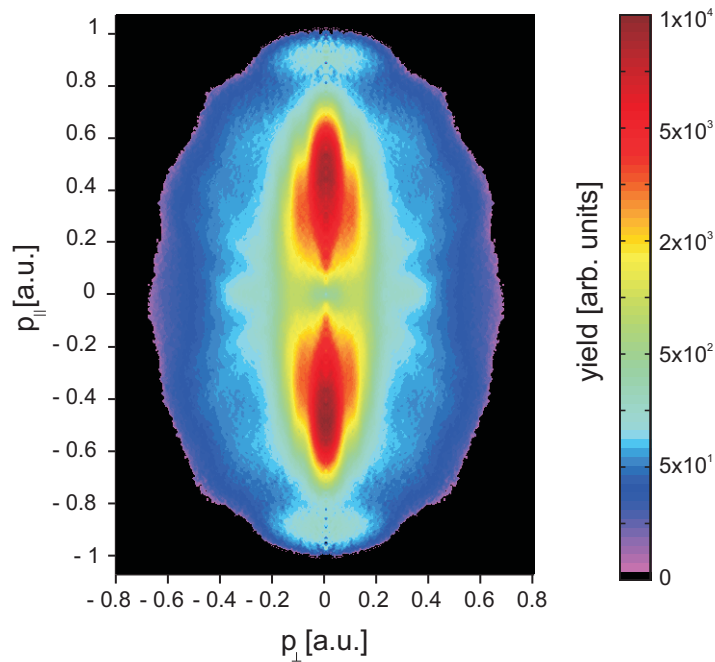


**Figure 3.** A cut through the CEP-averaged 3D momentum distribution of photoelectrons originating from the strong field ionization of xenon. Here,  $p_{\parallel}$  and  $p_{\perp}$  represent the momentum components parallel to and perpendicular to the laser polarization, respectively.

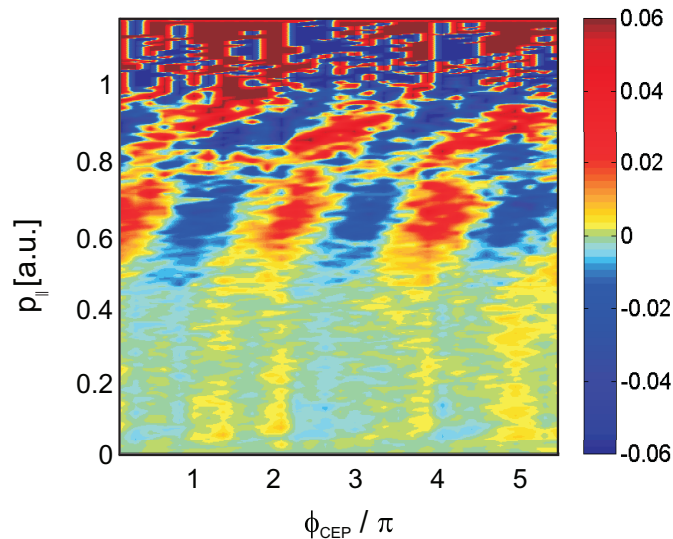


**Figure 4.** Asymmetry map  $A(|p_{\parallel}|, \phi_{\text{CEP}})$  obtained from the measured photoelectron spectra of xenon.  $\phi_{\text{CEP}}$  denotes the relative CEP, which differs from the absolute CEP by an arbitrary constant.

where  $N(p_{\parallel}, \phi_{\text{CEP}})$  denotes the yield of electrons with a momentum component  $p_{\parallel}$  in the interval  $[p_{\parallel}, p_{\parallel} + dp_{\parallel}]$ , measured for the CEP  $\phi_{\text{CEP}}$ . The up-down asymmetry map  $A(p_{\parallel}, \phi_{\text{CEP}})$  of the measured xenon spectra is displayed in figure 4. The asymmetry in the picture is color coded: red

corresponds to preferential emission in the upward direction, blue to preferential emission in the downward direction and green to symmetric emission of electrons in the up and down directions. For momenta  $p_{\parallel}$  between 0.5 a.u. and the cut-off at 1 a.u. a clear oscillation of the asymmetry with the CEP is observed. For a given momentum  $p_{\parallel}$ , the asymmetry has the form  $\cos(\phi_{\text{CEP}} + \delta(p_{\parallel}))$ , where  $\delta(p_{\parallel})$  is an additional phase that is a function of the momentum  $p_{\parallel}$ . At the onset of a hump around 0.8 a.u. the absolute value of the slope  $d\delta/dp_{\parallel}$  starts changing to a larger value at higher momentum. Interestingly, this phase jump at the interface between the low- and high-energy parts of the electron spectrum is similar to the phase jump we observed earlier in [20] in xenon at a wavelength of 760 nm. This indicates that these features have a common origin and are independent of the wavelength. The systematic investigation of the slope  $d\delta/dp_{\parallel}$  for different laser intensities will be the subject of a future study, but is beyond the scope of the present paper.

In conclusion, we have presented the first demonstration of the sub-cycle light-wave control of electrons at mid-IR carrier wavelengths using an intrinsically phase-stable laser source. CEP-dependent asymmetry was observed in the photoelectron spectra of xenon. We found that the CEP of pulses generated by OPCPA remains extremely stable for many hours of acquisition without the need for an active slow-loop stabilization. This conclusion is drawn from the fact that we did not observe any CEP jump in the recorded asymmetry maps during many consecutive hours of data acquisition, even when the acquisition time for a single asymmetry map lasted for about 1 h. The results of this proof of principle experiment open up a new horizon for the study of the attosecond dynamics of atoms and molecules in the mid-IR. In particular, they pave the way towards time-resolved studies of ultra-fast processes initiated by high-energy excitation.

## Acknowledgments

We acknowledge Marc Vrakking for support and for making specialized equipment available to us. We are grateful to the DFG for support via the Emmy-Noether program and the Cluster of Excellence: Munich Center for Advanced Photonics (MAP). RK acknowledges funding from a Sofja Kovalevskaja Award of the Alexander von Humboldt Foundation and an ERC Starting Grant.

## References

- [1] Krausz F and Ivanov M 2009 *Rev. Mod. Phys.* **81** 163
- [2] Brabec T and Krausz F 2000 *Rev. Mod. Phys.* **72** 545–91
- [3] Corkum P B 1993 *Phys. Rev. Lett.* **71** 1994–7
- [4] Paulus G G, Becker W, Nicklich W and Walther H 1994 *J. Phys. B: At. Mol. Opt. Phys.* **27** L703
- [5] Huillier A L and Balcou Ph 1993 *Phys. Rev. Lett.* **70** 774
- [6] Macklin J J, Kmetec J D and Gordon C L 1993 *Phys. Rev. Lett.* **70** 766
- [7] Meckel M *et al* 2008 *Science* **320** 1478–82
- [8] Drescher M *et al* 2002 *Nature* **419** 803
- [9] Kling M F *et al* 2006 *Science* **312** 246
- [10] Goulielmakis E *et al* 2008 *Science* **320** 1614
- [11] Telle H R *et al* 1999 *Appl. Phys. B* **69** 327–32
- [12] Jones D J *et al* 2000 *Science* **288** 635–9

- [13] Apolonski A *et al* 2000 *Phys. Rev. Lett.* **85** 740–3
- [14] Baltuska A *et al* 2003 *Nature* **421** 611–5
- [15] Helm H, Bjerre N, Dyer M J, Huestis D L and Saeed M 1993 *Phys. Rev. Lett.* **70** 3221
- [16] Gu X *et al* 2009 *Opt. Express* **17** 62
- [17] Baltuska A, Fuji T and Kobayashi T 2002 *Phys. Rev. Lett.* **88** 133901
- [18] Ghafur O *et al* 2009 *Rev. Sci. Instrum.* **80** 033110
- [19] Bordas C *et al* 1996 *Rev. Sci. Instrum.* **67** 2257
- [20] Kling M F *et al* 2008 *New J. Phys.* **10** 025024